Artificial Intelligence for Transportation 3–4 (2025) 100037

Contents lists available at ScienceDirect

Artificial Intelligence for Transportation

journal homepage: www.elsevier.com/locate/ait

Machine learning-based bicycle delay estimation at signalized intersections using sparse GPS data and traffic control signals - A Dutch case study using random forest algorithm

Yufei Yuan [a,*], Kaiyi Wang [b,*], Dorine Duives [a], Winnie Daamen [a], Serge P. Hoogendoorn [a]

[a] Department of Transport and Planning, Delft University of Technology, Delft, The Netherlands
[b] School of Business, The University of Queensland, Brisbane, Australia

ARTICLE INFO

Keywords:
Machine learning
Bicycle
Delay
GPS
Sparse
VLOG data
Random forest

ABSTRACT

Bicycle delay is an important variable to assess the performance of the cycling transportation system, especially as an indicator of intersection efficiency. This article estimates a machine learning (ML)-based model for estimating average bicycle delays at signalized intersections. This study evaluates various ML models with regressor features, including random forest, k-nearest neighbor, support vector regression, extreme gradient boosting, and neural networks. Sparse GPS cycling data (as reference data) from the Talking Bikes program in the Netherlands and the local control signal and flow detection information from the VLOG data provided by a Dutch city are adopted to train the ML models. The findings illustrate the viability of estimating bicycle delays by considering the interplay among weather conditions, temporal factors, junction topology, and local traffic conditions. The estimation model fit using the best-performing model - random forest - has doubled compared to the case without such additional traffic information, indicating its improved performance. Insights gained from the estimation model emphasize the potential of data-driven approaches to inform traffic management, bicycle policy, and infrastructure development.

1. Introduction

In modern urban mobility, bicycles have experienced a renaissance, emerging as a focal point for daily commutes and strategic urban policy. This revitalization in cycling has been spurred by the emergence of e-bikes and the global behavioral shift prompted by the COVID-19 pandemic, which has led to a surge in bicycle usage, as documented in recent studies (Younes et al., 2023). Bicycles are now heralded in policy circles as an eco-friendly replacement for cars, especially for short to medium-range urban trips.

This policy shift is evidenced by a trend among metropolitan areas worldwide to limit car traffic in city centers, aiming to reduce carbon emissions and reclaim space for pedestrians and cyclists. Bicycles are not only being integrated as a key component of urban transport networks but are also pivotal in bridging the gap in first/last mile connections to public transportation. Fraser and Lock (2010) further suggests that the integration of bicycles into the urban fabric extends beyond environmental benefits, touching on public health and socioeconomic factors (Fraser & Lock, 2010).

Recognizing these multifaceted advantages, there has been a concerted push by governments, including incorporating advanced cycling infrastructure, secure bike parking at transit nodes, and robust promotional initiatives advocating for cycling. Such strategic investments and campaigns are increasingly recognized for their potential to significantly elevate cycling as a preferred mode of transportation, as exemplified by the progressive policies and infrastructure in places like the Netherlands, which has become a global benchmark for cycling integration. Besides, historically car-oriented cities, like Washington D.C., the US, and Frankfurt am Main, Germany, successfully increased bicycle trip shares from the late 1990s to 2018 through strategic bike planning and policy implementation, demonstrating that even car-centric urban areas can promote cycling effectively (Buehler et al., 2021).

Bicycle-friendly cities are victims of their success. Unfortunately, our understanding of bicycle flow remains in its infancy compared with the seven decades of research and data collection on car-centric networks, which hinders the smooth integration of cycling into urban spaces in a safe and sustainable manner. Increasing cycling demand poses pressure on entire city networks. Ensuring precise determination of average delays, travel times, and stops for all road users, including vehicles, bikes, and pedestrians, is paramount in effectively managing signalized intersections at local and network levels (Bagdatli & Dokuz, 2021). Particularly, understanding delays has tangible implications for cyclists' daily

* Corresponding authors.
E-mail addresses: y.yuan@tudelft.nl (Y. Yuan), kaiyi.wang@student.uq.edu.au (K. Wang).

https://doi.org/10.1016/j.ait.2025.100037
Received 28 July 2025; Received in revised form 10 November 2025; Accepted 12 November 2025

Declarations

List of abbreviations

AI	Artificial intelligence
Det	Detection
KNMI	Royal Netherlands Meteorological Institute
LR	Linear regression
KNN	K-nearest neighbor
MAE	Mean Absolute Error
MAPE	Mean Absolute Percentage Error
MSE	Mean Square Error
ML	Machine learning
NN	Neural networks
RF	Random forest
RMSE	Root Mean Square Error
SHAP	Shapley Additive explanations
SVR	Support vector regression
XGBOOST	Extreme gradient boosting

lives. Excessive or unpredictable delays can discourage cycling for commuting, increase the likelihood of red-light running (Yang et al., 2012), and reduce overall travel time reliability. Such effects impact both commuters and recreational cyclists, influencing route choice, safety, and ultimately the attractiveness of cycling as a sustainable mode of transport as when delays are perceived as too long, cycling becomes a less appealing choice (Ton et al., 2017). Therefore, accurately quantifying bicycle delay is essential not only for traffic signal optimization but also for supporting broader goals of cycling promotion, urban livability, and sustainable mobility.

While field studies are a conventional means to gather this information, they can prove costly and time-consuming. Analytical methods, commonly employed for estimating delays, often struggle to generate accurate results, especially in scenarios of oversaturated traffic flow (Bagdatli & Dokuz, 2021). Alternative approaches are wanted that can provide more dependable and efficient estimates with minimal effort. Recently, delay estimation models based on artificial intelligence (AI) have been introduced in the literature to estimate delay more accurately and to simplify the relations amongst complex, influential factors to infer this crucial quantity. However, these applications have primarily focused on vehicular traffic (Bagdatli & Dokuz, 2021; Cheng et al., 2016). Cyclist and car traffic behavior are quite different, hampering the transferability of traffic algorithms initially developed for road traffic management. In addition, cyclist trips are underreported in most travel surveys or monitoring systems, which makes estimating bicycle demand and delay even more challenging due to limited cycling data quantity and quality.

Besides, the feed data for traffic state estimation models ranges from camera reading (automatic image processing or manual counting) to GPS data (either from a smartphone GPS module or from on-bike trackers/Apps). The former data source might provide the ground truth information, but the data extraction process is time-consuming and complex; the latter one might only provide a subset of the total traveler population (Yang et al., 2016). As an example, the Talking Bikes program (Mobiliteits-Platform, 2020) has been operational in recent years in the Netherlands, collecting GPS data and simultaneously integrating it with the broader “Talking Traffic” initiative. The outcome of the Talking Bikes program is a comprehensive dataset of GPS cycling data (from Apps or bike trackers), with over one million bicycle trips per year geographically distributed across the Netherlands. While the overall dataset size is substantial, it is worth noting that the distribution of trips at specific intersections may be limited, next to its data scarcity features regarding reporting frequency and duration.

Moreover, analytical estimation models require site-specific traffic control factors and demand information. This data category from signalized intersections is, for instance, in the Netherlands, available in the form of the VLOG format (Vialis, 2020). Note that this data is not generally available in a national database but might be available at a local scale. The VLOG data contains data on the control phase of traffic lights for motorized vehicles, cyclists, pedestrians, buses, and trams. Furthermore, data from several detection sensors (such as inductive loops/cables on vehicular roads, bicycle paths, and dedicated bus/tram lanes, request-green buttons for cyclists and pedestrians) near the intersection is available. This information is deemed to possess a close correlation with bicycle delays.

In this work, we develop and test a machine learning-based framework for identifying average bicycle delays at signalized intersections, using the relatively sparse GPS cycling data from the Talking Bikes program, the local control signal and flow detection information from VLOG data provided by the municipality of Delft, the Netherlands, and other contextual variables such as weather and temporal features. The proposed estimation model directly addresses the challenge of limited cycling data quantity and quality, demonstrating that meaningful delay patterns can still be captured under realistic data constraints. Its outcomes provide actionable insights for both signal optimization, traffic management and broader cycling policy. Compared with the authors’ previous work, this work enhances the capabilities and generalizability of the bicycle delay estimation model by incorporating newly added VLOG traffic control data, thereby offering a more robust and transferable modeling approach.

The remainder of this paper is organized into five sections. Section 2 presents the related work for data-driven bicycle delay estimation methods for signalized intersections. Section 3 elaborates on the research methodology, including the conceptual framework and an introduction to the model approaches. This is followed by Section 4, which describes the case studies for estimating bicycle delays at signalized intersections. Section 5 presents the modeling results and discusses to what extent the case study validates the proposed concept. Finally, Section 6 concludes the paper with a summary of the main findings and some recommendations.

2. Related work to capture traffic delays

Many studies have investigated vehicle delays at signalized intersections (Bagdatli & Dokuz, 2021; Cheng et al., 2016). Vehicles experience three types of delay at signalized intersections: control delay, stop delay, and approach delay. Control delay is expressed as the total delay caused by the intersection control, including deceleration, stop, and acceleration delay. Stop delay is defined as the duration in seconds that traffic users are forced to stop at an intersection. Approach delay occurs from a predefined upstream point to the intersection stop line. This definition and concept are commonly employed in describing vehicle delays (Cheng et al., 2016), and we posit that a similar framework applies to bicycle traffic.

Only a limited number of studies have concentrated on cycling delays at signalized intersections, whether wholly or partially. These studies primarily depend on analytical methods to deduce observed delays based on bicycle trajectories. For instance, Velthuijsen (2020) directly calculated and estimated bike delays from smartphone GPS data in a Dutch city based on fundamental physics law (Velthuijsen, 2020). This study considers three scenarios of defining reference speed values (as the ‘free-flow’ speed). Similarly, Rupi et al. (2020) and Poliziani et al. (2022) inferred bicycle waiting times (including delays) based on a predefined threshold speed, using relatively rich GPS traces at a city scale in Italy (Poliziani et al., 2022; Rupi et al., 2020). The novelty of these studies lies in a pre-processed map-matching operation to enhance estimation accuracy. Gillis et al. (2020) measured bike delays at signalized intersections by interpolation between GPS locations before and after the intersections (Gillis et al., 2020), relying on data from the Bike Count Week in Belgium (Lancering Nationale FietsTelWeek 2015, 2015). A similar approach to deriving delay times can be

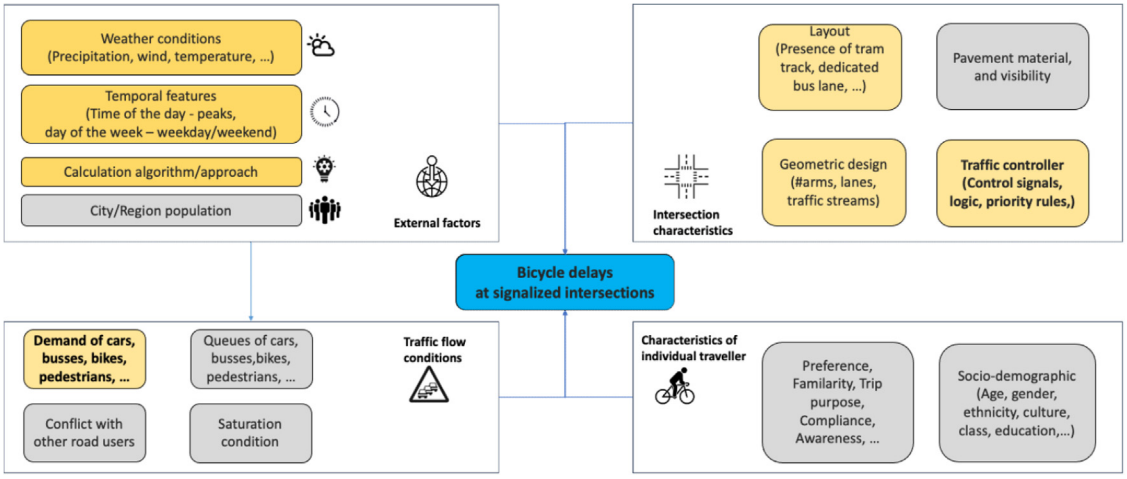

Fig. 1. Conceptual framework of bicycle delays at signalized intersections. The highlighted influential variables are included as the independent variables in this work.

found in studies in Canada (Strauss & Miranda-Moreno, 2017) and Sweden (Kircher et al., 2018). However, these studies did not develop specific estimation models to capture and reproduce typical delay patterns.

Yuan et al. (2019) developed a linear regression model to estimate the start-up lost time as part of approach delay (which is used to calculate bicycle flow capacity at intersections) from empirical trajectory data derived from cameras at a specific intersection in Amsterdam (Yuan et al., 2019). Few attempts have been made to utilize ML models for bicycle delay estimation and inference. Reggiani et al. (2020) successfully employed a neural network model to estimate individual cyclist travel times, considering various scenarios, including approach delay, stop delay, and/or control delay (Reggiani et al., 2020). Their study utilized data from cameras, loop detectors, and control signals in a Dutch city-Utrecht. Previous work mainly applies a single model. Yuan et al. (2023) have demonstrated the feasibility of estimating bicycle delays via multiple ML models using only sparse GPS cycling data and publicly accessible information, leveraging the burden of understanding local traffic conditions (Yuan et al., 2023). The work shows that understanding the role of temporal/ weather variables and turning typology can help in planning for expected/predicted delays during certain times/conditions and can inform strategies to manage and reduce such delays at specific intersections or on a national level. While ML has shown considerable promise in improving traffic state estimation, its utilization for bicycle delay estimation is still rare, particularly in situations where sparse GPS data and traffic controller information are both involved. This study aims to address this research gap.

3. Methodology for bicycle delay estimation

This section presents the research methodology that enables us to estimate the bicycle delay at a signalized intersection. This section first describes the modeling conceptual framework. It is followed with a presentation of the set of mathematical models used to capture the intersection delay, the training procedure and the performance. Accordingly, a description of the datasets is provided, including the definition of both the dependent and independent variables.

3.1. Conceptual framework to capture bicycle delay

We have developed a conceptual modeling framework of all the most relevant factors based on findings in the literature and authors' assumptions (Yuan et al., 2023) to explain bicycle delays at intersections, as shown in Fig. 1. Four categories are identified: characteristics of individual travelers, intersection characteristics, traffic flow conditions, and external factors. In the context of this work, the characteristics of intersections are identified as an important attribute. The geometry design, layout, pavement, and visibility will influence how cyclists interact with other road users and the environment. The controller scheme (e.g., signals, logic, priority rules) contributes the most to the stop and control delays at signalized intersections. Besides, the local traffic conditions need to be considered, such as the demand and queue length of various transport modes, saturated or oversaturated, because the control signals may assign more green times to the mode with priorities.

In this article, we extend our previous work (Yuan et al., 2023) by additionally including local control signals and traffic count information to enhance estimation capability. Local control signals provide detailed information about signal timings and phase sequences specific to each intersection. Count information includes the number of bicycles and other road users passing through the intersection. Incorporating this data is assumed to enhance the performance of delay estimations. Therefore, the underlying datasets include sparse GPS cycling data, meteorological data, temporal information, intersection topology, turning typology, and newly added intersection control signal and count information. It should be emphasized that our primary goal is not to develop the most precise estimation model for real-time monitoring of bicycle delays on a per-movement basis at signalized intersections. Instead, our focus is on optimizing the utilization of existing data sources, considering their quality and capabilities, to extract valuable insights for traffic management.

3.2. Mathematical model description

This work will apply the same set of ML estimation models as in Yuan et al. (2023), ranging from simple linear regression (one of the most popular econometric models) to sophisticated machine-learning approaches. Based on the characteristics of the dataset variables, we initially selected five widely recognized machine learning models equipped with regression capabilities to address the problem at hand. These include random forest (RF), k-nearest neighbor (kNN), support vector regression (SVR), extreme gradient boosting (XGBoost), and neural networks (NN). Note that the five chosen ML models have indicated their validity for vehicle delay estimation to capture temporal trends and physical processes (Bagdatli & Dokuz, 2021; Cheng et al., 2016). However, they have not yet been widely applied in the literature for bicycle traffic state estimation at signalized intersections.

• Random Forest (RF)

Random Forest stands out as a multi-faceted machine learning technique adept at both regression and classification tasks (Biau & Scor-

net, 2016). This method harnesses the power of ensemble learning, where a collection of simple models, or "weak learners," are united to create a strong, more predictive model. This approach is particularly suitable for delay prediction due to its ability to handle many input variables and its robustness to outliers, which is typical in urban cycling data. It can effectively capture the non-linear and complex interactions between various factors influencing bicycle delays.

• k-Nearest Neighbors (kNN)

The k-Nearest Neighbors algorithm operates on a principle of proximity, making it an intuitively simple yet effective method for classification and regression (Leif, 2009). It assigns outputs based on the predominant outcome or the mean of the 'k' closest instances in the training data. This proximity is quantified using distance metrics such as the Euclidean or Manhattan distance, providing a straightforward mechanism for pattern recognition. This algorithm relying on proximity could be helpful in modeling delays, which can be highly localized and influenced by nearby traffic conditions. Its simplicity also allows for quick adjustments to the model as new data becomes available.

• Support Vector Regression (SVR)

Support Vector Regression, a regression-focused offshoot of Support Vector Machines (SVM), tackles both linear and nonlinear regression tasks (Smola & Schölkopf, 2004). SVR operates by mapping data to a higher-dimensional feature space and determining the optimal hyperplane that remains within a predefined error margin, effectively balancing the model's complexity with its predictive prowess. The capacity to find a hyperplane that best fits the data makes it a good choice for delay estimation, where the goal is to predict continuous delay times. It is adept at managing the complexities of urban traffic data and can handle non-linear patterns effectively.

• Extreme Gradient Boosting (XGBoost)

Extreme Gradient Boosting is renowned for being a potent and fast machine learning algorithm, particularly in regression and classification domains (Chen & Carlos, 2016). It refines the concept of gradient boosting by optimizing existing models and incrementally reducing errors through its 'weak learners.' This results in a highly performant and scalable model that is a favorite among data scientists for its efficacy. XGBoost is suitable due to its high performance and speed, which are essential in processing and analyzing large volumes of cycling data in real time. Its ability to do feature engineering autonomously helps identify the most significant factors affecting bicycle delays.

• Neural Networks (NN)

Neural Networks, inspired by the neural structures of the brain, excel in detecting patterns and processing complex sensory data (Goodfellow et al., 2016). These networks adeptly categorize or cluster inputs, undergoing training to discern complex patterns and output predictions or decisions that mimic human cognitive processes. They are especially powerful in situations where the input variables are tightly linked to the predicted outcomes, making them invaluable tools in the machine learning field. Thanks to their deep learning capabilities, NNs are well-suited for capturing the intricate relationships within cycling data. They can model the complex interactions of traffic dynamics that traditional models might miss, thus providing a more accurate prediction of bicycle delays.

3.3. Model training procedure

The predictors (independent variables) are stored in 'X', while the target dependent variable is stored in 'y'. To divide the data into training (80 %) and testing (20 %) subsets, we employed a stratified sampling technique, using intersection identifier ('Intersection_ID' in Table 1) as the stratification criterion to ensure a proportional representation of all intersections across both datasets. Consequently, each dataset reflects a balanced cross-section of intersections.

We developed a bicycle delay estimation model, employing multivariate linear regression as the benchmark due to its simplicity and interpretability. The model was trained using a designated training dataset, and we investigated the relevance of various features to travel delays by analyzing their respective P-values. The other five ML models were tuned and trained using a grid search strategy in combination with the 5-fold cross-validation. Gird search can ensure clarity and transparency in hyperparameter tuning, though this method can be computationally expensive. More advanced approaches such as 'Hyperopt' or randomized search could improve efficiency, and we intend to explore these in future work with larger datasets. Cross-validation is a robust statistical technique that helps prevent model overfitting by partitioning the data into subsets, training the model on a subset, and then validating it on the remaining data (in this case – 5 folds are created, the method trains and evaluates the model 5 times, picking a different fold (20 %) for evaluation every time and training on the other 4 folds (80 %)). 5-fold cross-validation is commonly used because it strikes a balance between providing a stable estimate of model performance and maintaining computational efficiency, unlike lower values of folds that may yield more variable results and higher values that require more computational resources (Brownlee, 2020). This approach ensures the model's generalization ability, enhancing its predictive performance on unseen datasets, thus strengthening the reliability and credibility of the study (Aurélien, 2019). Considering our dataset's extensive temporal range (of over two years), we anticipate that the randomly constituted training sets will encompass a comprehensive array of the characteristics (both in space and time) in the overall sample population.

This systematic exploration and evaluation of numerous hyperparameter combinations aimed to optimize the predictive performance of the models. The best scores achieved from the grid search, a machine learning technique that methodically works through multiple combinations of parameter tunes, cross-validating as it goes to determine which tune gives the best performance, are reported in the subsequent section corresponding to the lowest error rates. Note that all the estimation models were written and interpreted in Python using the 'scikit-learning' package. (see: https://scikit-learn.org/stable/user_guide.html, accessed on 1 Jan, 2024).

3.4. Model performance indicators

In the evaluation of the estimation models, two key performance indicators, R-squared (R^2) and Root Mean Square Error (RMSE), are employed to assess the model's predictive accuracy and reliability for both training and testing sets. The R-squared metric, also known as the coefficient of determination, quantifies the proportion of the variance in the dependent variable (bicycle delay) that is predictable from the independent variables. This metric measures how well-observed outcomes are replicated by the model based on the proportion of total variation of outcomes explained by the model. A higher R^2 indicates that the model's estimation aligns more closely with the observed data, signifying a more accurate model.

RMSE, on the other hand, measures the average magnitude of the prediction error, i.e., the differences between the predicted and observed values. It quantifies the model's predictive error, which is directly linked to the concept of reliability. A smaller RMSE indicates a model that reliably produces less error, implying better reliability. Furthermore, because RMSE penalizes larger errors more severely, models that minimize RMSE are especially desirable when large prediction errors are particularly problematic. In contrast, metrics like MAE (Mean Absolute Error) would provide less significant penalization for larger errors; MSE (Mean Square Error) does not provide the intuitive scale as RMSE does; MAPE (Mean Absolute Percentage Error) can heavily penalize minor deviations when the actual values are low, which is not

Table 1
Overview of influential variables used in the machine learning models.

	Predictors	Data type	Details	Example data entry
Intersection identifier	Intersection_ID	Integer	Intersection index	1
Weather conditions	Precipitation_Duration	Integer	Duration of precipitation in s over 10 min	600
	Precipitation_Intensity	Decimal	Precipitation intensity over 10 min (mm/h)	2.41
	Temperature	Decimal	Average air temperature in °C over 10 min	13.30
	Wind_Average_Speed	Decimal	Average wind speed in m/s over 10 min	8.47
	Wind_Maximum_Speed	Decimal	Max. actual wind speed in m/s over 10 min	12.43
Temporal features	Weekday_Number	Integer	Day of the week of the travel record (with 1 denoting Sunday, 2 denoting Monday, and so forth until 7 [Saturday])	1
	Hour	Integer	Hour of the day of the travel record	13
	Peak_Dummy	Dummy	Peak hour indicator (1: peak for the period between 7:00 and 19:00; 0: otherwise)	1
Control signal VLOG data	Car detection	Integer	Summation of all car counts (signal pulses) for all detectable directions per interval (5 mins)	20
	Bus/Tram detection	Integer	Summation of all bus/tram counts (signal pulses) for all detectable directions per interval (5 mins)	10
	Bike detection (request-green button and loop detection)	Integer	Summation of all bike counts (push frequency, and signal pulses) for all detectable directions per interval (5 mins)	10
	Pedestrian detection (request-green button)	Integer	Summation of all pedestrian counts (pulses) for all detectable directions per interval (5 mins)	10
	Car signal duration	Decimal	Relative green time per interval (5 min = 300 s)	0.15
	Bus signal duration	Decimal	Relative green time per interval (5 min = 300 s)	0.15
	Bike signal duration	Decimal	Relative green time per interval (5 min = 300 s)	0.15
	Pedestrian signal duration	Decimal	Relative green time per interval (5 min = 300 s)	0.15
Intersection characteristics	Stream_No.	Integer	Standard index of bike flow movements at intersections (1, 2, 3, …, 12)	2
	Arms	Integer	Total No. of arms	4
	Car_Lanes	Integer	Total No. of car lanes	12
	Bike_Streams	Integer	Total No. of bike streams	12
	Tram_Dummy	Dummy	The presence of the tram line (1: presence)	1
	Bus_Dummy	Dummy	The presence of the bus lane (1: presence)	0

ideal for our application. Therefore, they are not selected as error indicators. This study applied a log transformation (the natural logarithm of one plus the input array) to improve the model's performance to the delay outcome variable. This transformation serves to temper the influence of extremely high values, resulting in a more symmetrical distribution and, thus, more amenable to modeling (West, 2021). However, due to this transformation, interpreting the R-squared and RMSE values should be cautiously approached as they now represent relationships in the log scale (West, 2021). Additionally, to assess the statistical significance of performance improvements across scenarios, a paired *t*-test was conducted on the prediction errors using the same training or testing datasets. We tested the prediction errors across scenarios using the paired *t*-test, confirming the statistical significance of the difference/improvement.

A comparative analysis of the distribution of the predicted and original delays was conducted using the testing set to assess the model performance further. This involved visualizing the distributions of both data sets to observe any differences or similarities. Given the significant right-skewed distribution of the data, the median was chosen as a more robust measure of central tendency compared to the mean. Therefore, the medians were compared to provide a more accurate representation of the central location of the data. This approach helps to mitigate the influence of outliers and provides a more reliable comparison between the predicted and actual values for average delays and specific delays per movement direction.

3.5. Description of the GPS dataset

The collected GPS cycling data records changes in locations and time instances without differentiation based on individual transportation modes or motives which is in line with General Data Protection Regulation (GDPR) in Europe. The trip samples encompass cyclists utilizing bike Apps (such as Ring-Ring (Mobiliteits-Platform, 2020)), shared bike users, or company bike users (via bike trackers like Tracefy (Mobiliteits-Platform, 2020)), amounting to approximately 3 million bicycle rides without sociodemographic detail across the country within a two-year span. While the dataset's overall size is considerable, it is essential to acknowledge that the distribution of trips at specific intersections over two years may be limited. On average, there are around 4000 collected daily trips distributed across the country. The sampling rate varies by trip and data record due to occasional connectivity loss, ranging from 1 s to 30 s with a median data density of 7 reporting points and median trip durations ranging from 407 s to 552 s, justifying this GPS dataset's inherently 'sparse' and 'imperfect' nature. Note that we use the 'raw' dataset from the Talking Bikes Program without additional refinement or pre-processing using data augmentation and imputation strategies (e.g., map-matching techniques as applied in Gao et al. (2024)). The current dataset and its derived variables are used as the reference for this analysis. These data imperfections (i.e., scarcity, irregular sampling) reflect real-world data collection variability and partly explain the upper bound in achievable model performance under real-world data conditions.

3.6. Delay definition (dependent variable)

In the conventional delay analytical approach, three delay types are distinguished. The delay event contains processes distinct from each other and has a multidimensional and nonlinear nature. The current 'sparse' GPS data cannot capture all these details, such as when a cyclist passes the stop line of a specific arm, which can be used to compute, e.g., stop delay and approach delay. The VLOG data can only partially reflect control delay; besides, identifying accurate control delay experienced by individual travelers for specific movement directions is a challenging task. In our previous work, we have creatively developed a method to define the travel time and, thus, the experienced bicycle delay to compensate for the data incompetency (Yuan et al., 2023).

The experienced delay (as 'DelayTime') is defined as the difference between the observed travel time (excluding activity travel time (Hoogendoorn, 2005; Yuan et al., 2016) and the free-flow (or desired) travel time for a specific path that follows the trajectory from the up-

stream arrival location to the downstream departure location at the intersection (e.g., turn left/right or cross straight ahead). The central assumption is that this delay can cover all the delay components experienced by cyclists passing an intersection.

With GPS data's longitude and latitude coordinates, we can derive the elapsed time (duration) between a detectable upstream GPS location and a detectable downstream GPS location of the intersection, considering the observed travel time of individual rides. These observed travel times are considered the actual travel times experienced by cyclists for reference (as the ground truth for estimation models).

The free-flow travel time is calculated as the travel distance between the upstream and downstream GPS locations divided by a predefined free-flow cycling speed (in this work, the value is set as 4 m/s - obtained from the literature (Balevski & Lyubenov, 2018; Guo et al., 2021)). Note that this fixed value provides a standardized reference and isolates the effect of speed heterogeneity, and thus it may not reflect variations across different age groups or trip purposes.

Besides, we distinguish these travel time/delay samples according to their movement directions at intersections (numbered 1 to 12 clockwise; movements of 1,2,3 are labeled at the right-handed (eastern) side of the intersection). Given the relatively sparse data samples, we categorize cycling movements into three main groups: right turns - R (movements 1, 4, 7, 10), through-going - T (movements 2, 5, 8, 11), and left turns - L (movements 3, 6, 9, 12), due to their specific movement features (e.g., cyclists turning right do not have to stop).

3.7. Description of the independent variables

The highlighted factors, as shown in Fig. 1, will be included in our estimation models, including intersection characteristics (control signals and detection information per traffic mode from VLOG data (available for this research), intersection layout, and external factors (weather information from KNMI and temporal messages). The detailed information is further elaborated in Table 1. Specifically, the features are further described as follows:

• VLOG data

The VLOG data contains data on the control phase of traffic lights for motorized vehicles, cyclists, pedestrians, buses, and trams. Furthermore, data from several detection sensors (such as inductive loops on vehicular roads and bicycle lanes, request-green buttons for cyclists and pedestrians during red) near the intersection is available, see an example in Fig. 2. This information is assumed to correlate strongly with observed delays experienced by cyclists (and our result will prove this assumption).

In particular, concerning the count information, for a generic application, we aggregate all counts (number of times the button was pushed, number of cable-occupied periods) per mode across all detectable movement directions per output interval. This approach aims to isolate the heterogeneity inherent in intersection detection configurations. Similarly, we normalize control signal times per mode as model input, specifically by averaging relative green time for all available streams per mode within each output interval set at 300 s (the same as the default output interval in the VLOG data). Please note that the count information can only partially reflect the total traffic demand at intersections, as it may involve instances of undercounting or double counting. Therefore, caution should be exercised when interpreting this absolute value.

• Intersection characteristics

Several intersection design features are considered during the ML model training, such as the number of arms, car lanes, available bike movement streams, and their corresponding stream numbers using standard directional codes. Additionally, dummy variables are incorporated to indicate the presence of tram and bus lanes. For a detailed example, please refer to the next section.

• Temporal features

Temporal factors are also assumed to play a role in our analysis, and we have included three features: weekday number, travel hour, and a peak hour indicator. Note that the case study comprises a total of 504 trips (Table 2), with the highest number observed on Tuesdays (90 trips) and the lowest on Saturdays (48 trips), averaging 72 trips per day, with 58 % occurring during peak hours.

• Weather data

We considered precipitation, temperature, and wind variables in our initial exploration of weather data as a potential determinant for bicycle delays. We sourced public open weather data from the Royal Netherlands Meteorological Institute (KNMI) Data Platform, downloading and combining the ASCII data files. Upon reviewing the GPS coordinates of the weather observatories, we selected to include data from several locations nearest to our specified intersections. These include Voorschoten (for intersections at The Hague), Schiphol Location 18Ct (Amsterdam), Rotterdam Location 24t (Rotterdam and Delft), Eindhoven Location A (Eindhoven), and De Bilt Location A (Utrecht). Numerous weather variables were recorded in the merged dataset, from which we selected the most representative predictors potentially related to travel delay, as revealed in Yuan et al. (2023). These include precipitation duration and intensity, temperature, average, and maximum wind speed, as further elaborated in Table 1. The weather data provided primarily represents the real-time conditions observed at the weather stations. While these readings can be useful in predicting weather conditions at nearby intersections, such interpretations must be cautiously made. This is because the physical distance between the weather station and a given intersection can introduce discrepancies in the actual weather conditions present at the intersection. Within the total trips in the case study, general descriptive statistics for the five selected predictors are as follows: precipitation duration (mean = 67.6, std. = 178.8), precipitation intensity (mean = 0.15, std. = 0.77), temperature (mean = 11.4, std. = 5.5), and average and maximum wind speed (mean = 4.7 and 7.0; std. = 2.9 and 4.4, respectively).

• Correlation analysis

A correlation analysis was conducted to examine potential multicollinearity among the independent variables (based on the data in the case study), see Fig. 3. Overall, most predictors displayed modest correlations, suggesting that they capture distinct aspects of the cycling and traffic environment. Via this analysis, it is noticed that there exist high correlations between the average wind speed and max. actual wind speed (corr. $\approx$ 0.99), as well as bus detection and bus signal duration – relative green time per interval (corr. $\approx$ 0.87). Both cases reflect expected operational dependencies in weather data and control signal data. We intentionally keep the information to avoid information loss. Multicollinearity is a known issue in linear models, tree-based models like Random Forest are generally robust to multicollinearity and can accommodate interrelated predictors, as they do not rely on linear coefficients but instead use recursive binary splits. The observed correlations deserve caution in result interpretation related to these two variable pairs.

4. Case study description

This section describes the scenario setup, the configuration of the estimation models, and the assessment criteria.

Access to the datasets used in this study is highly constrained, as the Talking Bikes GPS data are available only through the Dutch Ministry of Transportation, and the VLOG signal control data are not part of any national database but were obtained only at a local scale. The data from (only) two busy cycling intersections in Delft (namely, a 4-armed intersection at Westlandseweg – Nieuwe Gracht – ID 1 and a T-junction

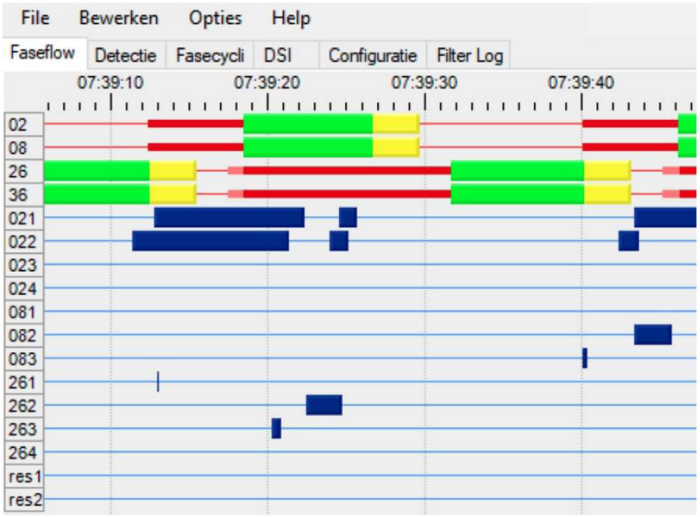

(a)

periode	21	22	23	24	81	82	83	261	262	263	264	res1	res2	02	08	26	36
07:30-07:35	12	7	7	9	5	5	5	28	5	16	12	0	0	67.4	67.4	107.6	107.6
07:35-07:40	14	4	6	6	2	1	3	44	10	12	13	0	0	54.3	54.3	161.5	161.5
07:40-07:45	21	7	11	15	3	3	6	37	9	19	11	0	0	72.3	72.3	127.8	127.8
07:45-07:50	23	8	12	19	5	5	6	26	19	17	8	0	0	92.7	92.6	103.3	103.2
07:50-07:55	20	10	10	16	10	10	11	28	14	17	17	0	0	97.3	97.3	78.3	78.3
07:55-08:00	33	9	20	27	10	9	9	73	12	23	13	0	0	95.8	95.3	100.8	100.3
08:00-08:05	22	11	15	19	17	15	17	43	14	19	17	0	0	108.5	108	79.3	78.8
08:05-08:10	20	11	15	16	19	16	19	83	17	21	16	0	0	97.3	97.3	91.4	91.4
08:10-08:15	16	7	11	15	14	15	16	66	13	17	18	0	0	87.4	87.4	103.9	103.9
08:15-08:20	16	8	13	13	13	12	12	44	14	17	16	0	0	80.1	80.1	117.6	117.6
08:20-08:25	21	8	14	17	10	9	9	46	19	23	15	0	0	78	78	121.3	121.3
08:25-08:30	17	6	8	10	11	9	11	67	21	27	17	0	0	80	80	121	121
08:30-08:35	12	13	7	7	9	10	12	100	28	30	11	0	0	78.5	78.5	116.5	116.5

(b)

Fig. 2. (a) A random VLOG sample visualized in CuteView software (Interstyles, 2021); (b) Recorded information of a random VLOG sample. Note, control signal IDs: 02, 08, 26, and 36; detection sensor IDs: 21, 22, 23, 24, 81, 82, 83, 261, 262, 263, and 264.

Table 2
Intersection characteristics and the related data sample size.

ID	#Arm	#Car lanes	#Bike Streams	Tram Dummy	Bus Dummy	#Trip Record
1	4	12	12	1	1	332
2	3	4	6	0	0	172

Note: # denotes number.

at Jaffalaan – Mekelweg – ID 2) are adopted. See Fig. 4 for a general impression of the intersection, and Tables 2 and Table 3 for their characteristics. These two intersections daily accommodate huge commuting cycling flows to the train station and the university (Delft University of Technology) of Delft, especially in peak hours before lectures start or after they end.

Both intersections feature no directional restrictions. Consequently, we can identify 12 movement directions for each of the two intersections. The municipality provided the corresponding information of traffic controllers at these two intersections as model input.

4.1. Scenario setup

To validate the proposed approaches, two scenarios are designed.

Scenario 1 considers using the data from one intersection (ID 1) (including control signals and detection information for cars, bikes, pedestrians, trams, and buses). Scenario 1 focuses on the standard 4-armed signalized intersection; we would like to test our assumption that incorporating the VLOG data can enhance the performance of delay estimations. To this end, we need to compare it with the scenario excluding the VLOG data. Therefore, there are two testing variants.

Scenario 2 adopts the data from two intersections (ID 1 and ID 2) with sacrificed data features to maintain consistency of input variables between the two intersections (excluding bus/tram signal, bus, and pedestrian detection). Scenario 2 extends the assessment of the estimation models' generalizability to additional intersections (ID2: T-Junction).

4.2. Model training procedure and parameter setup for the case study

In this study, we first separated the dataset into predictors (X) and the target variable (y). The predictors, stored in 'X', encompass all columns of the data except for 'DelayTime'. Conversely, 'DelayTime' was selected as the target variable and stored in 'y'.

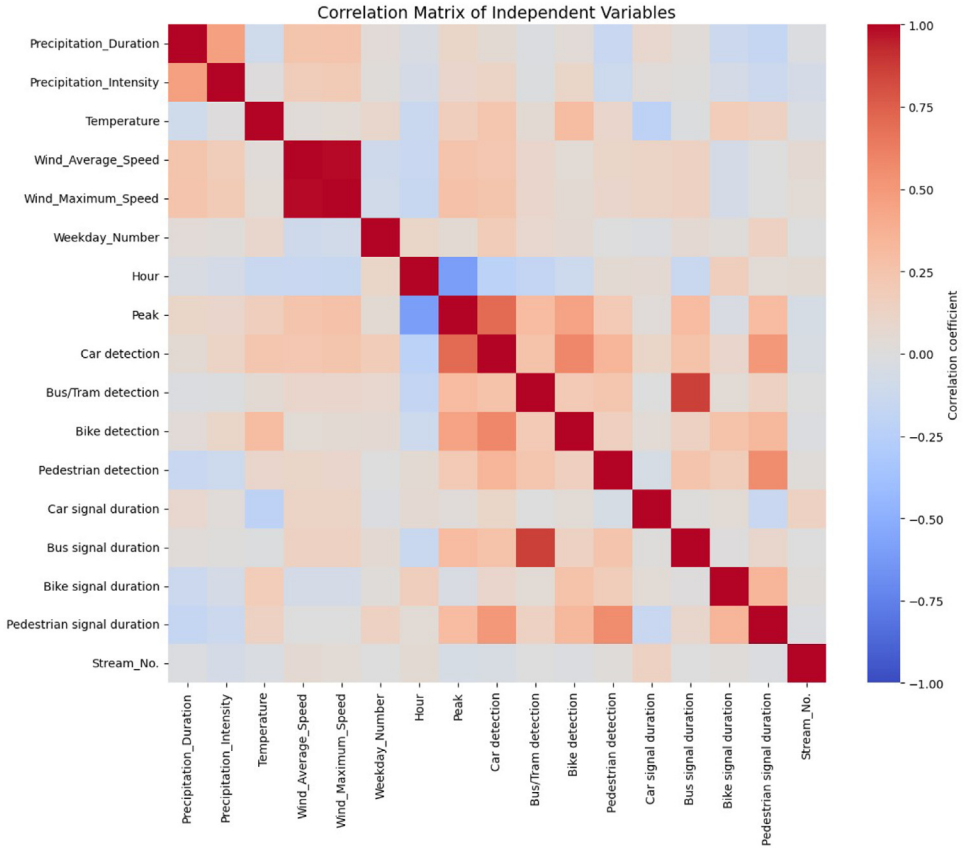

Fig. 3. Correlation heatmap for all independent variables adopted in estimation models (value range: −1∼+1).

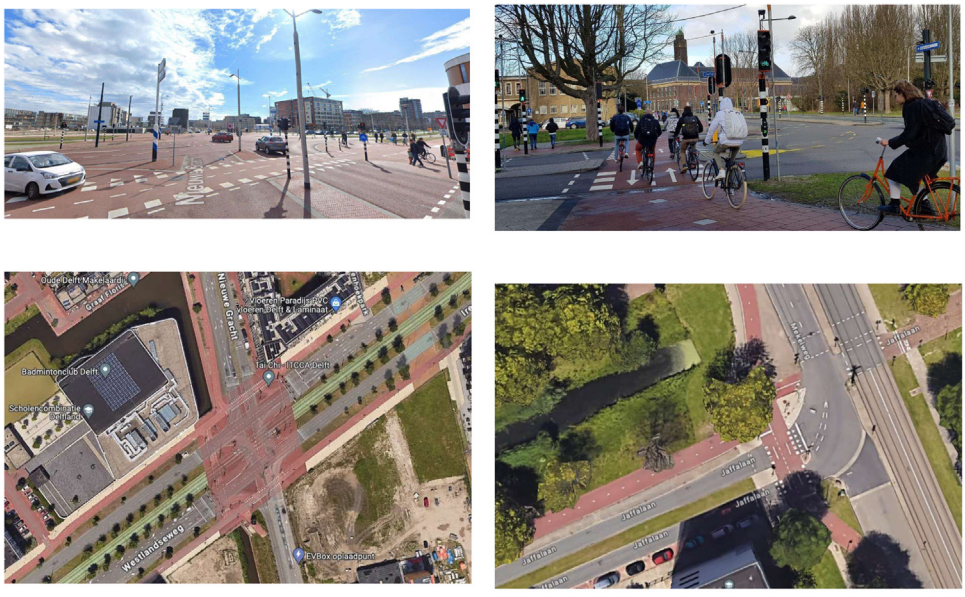

(a) ID 1 (b) ID 2

Fig. 4. Snapshots (top) and top view plans (bottom) of the intersections at Westlandseweg-Nieuwe Gracht (a) and Jaffalaan-Mekelweg (b) in the city of Delft.

Several tests of parameter turning have been conducted in this study after considering the successful applications in the literature. As a result of this fallacy process of a grid search, the most successful parameters were found in the models. This paper explicitly reports the optimized parameters for Scenario 1 and Scenario 2, each incorporating weather, temporal, and topology data, as well as the VLOG data, with the detailed outcomes provided in Table 4.

5. Results and discussion

This section begins by providing an overview of the overall performance of the two scenarios, followed by an examination of their respective performance in terms of feature importance and comparison of delay distributions. Specifically, in scenario 2 which benefits from its enhanced representativeness, taking into account space limitations, we

Table 3
Overview of VLOG data characteristics for the two intersections.

	Int. ID 1 - Westlandseweg – Nieuwe Gracht		Int. ID2 - Jaffalaan – Mekelweg	
	Availability	# items	Availability	# items
Car Det.	Yes	8	Yes	7
Bike Det. (loop + request)	Yes	6 + 6	Yes	2 + 2
Ped Det. (request)	Yes	16	No	0
Bus/Tram Det.	Yes	4	No	0
Car signal	Yes	10	Yes	2
Bike signal	Yes	6	Yes	1
Ped signal	Yes	8	Yes	1
Bus/Tram signal	Yes	4	No	0

Note: # denotes number; Det.: detection.

Table 4
Optimized parameters in the machine learning modeling process for Scenarios 1 and 2 with the VLOG data.

Algorithm	Scenario 1 Optimized parameters	Scenario 2 Optimized parameters
RF	n_estimators: 84 (the number of trees in the forest) criterion: Poisson criterion max_depth: 9 (the maximum depth of the tree) min_sample_leaf: 2 (the minimum number of samples required to be at a leaf node) min_samples_split = 1 (the minimum number of samples required to split an internal node)	n_estimators: 190 criterion: Poisson criterion max_depth: 12 min_sample_leaf: 6 min_samples_split = 1
XGBoost	n_estimators = 50 (the number of boosting stages to perform) max_depth = 2 (maximum depth of the individual regression estimators) min_sample_leaf = 1 (the minimum number of samples required to be at a leaf node) min_samples_split = 2 (the minimum number of samples required to split an internal node) learning rate = 0.1 (the rate shrinks the contribution of each tree)	n_estimators = 100 max_depth = 5 min_sample_leaf = 4 min_samples_split = 2 learning rate = 0.01
kNN	n_neighbors = 9 (number of neighbors to use by default for k neighbors queries) p_params: 2 (standard Euclidean distance) Weights: Uniform	n_neighbors = 9 p_params: 2 (standard Manhattan distance) Weights: Distance
SVR	Estimator_kernel = 'rbf' (the radial basis function) Estimator_gamma= 'scale' (kernel coefficient) *C* = 1 (a regularization parameter) epsilon = 0.1 (a parameter determines the width of the tube around the estimated function)	Estimator_kernel = 'rbf' Estimator_gamma= 'scale' *C* = 1 epsilon = 0.3
NN	hidden_layer_sizes: (50,50,50) (the number of neurons in the ith hidden layer) activation function = 'tanh' (the hyperbolic tan function) solver = 'sgd'(stochastic gradient descent.) learning rate = 'adaptive' (adaptive learning rate schedule for weight updates) alpha = 0.05 (Strength of the L2 regularization term)	hidden_layer_sizes: (50,50,50) activation function = 'tanh' solver = 'sgd' learning rate = 'constant' (constant learning rate schedule for weight updates) alpha = 0.0001

Note: RF: random forest; XGBoost: extreme gradient boosting; kNN: K-Nearest Neighbors; SVR: support vector regression; NN: neural networks.

conduct a detailed SHAP analysis to explore the influence of model features. The section concludes with a reflection on the pertinent insights gleaned for traffic management.

In the previous work (Yuan et al., 2023) employing the same model set and considering weather data, demographic, complexity, and temporal information (no VLOG data), the R^2 value of the best-performing model (the RF model) was approximately 10 % with a 1.092 RMSE score (log). This result was derived from training the model using data from 18 intersections from 6 representative Dutch cities. The RF model predicted bicycle delays based on multiple features outperforms the others due to the advantage of being robust to outliers and non-linear data. This finding is consistent with the previous application of vehicle delay estimation in Bagdatli and Dokuz (2021), where both RF and XGBoost techniques present their superiority. The RF model indicates that the temperature variable was the most influencing predictor in the training process (see Fig. 5). Other important features include the turning typology ('Stream_Number'), wind variables ('Wind_Maximum_Speed' and 'Wind_Average_Speed'), and temporal features (such as 'Hour', 'Day', and 'Weekday_Number').

5.1. Overall performance of the two scenarios

Aligned with earlier findings, the RF model is the most effective machine learning model in our training evaluations across both scenarios. Table 5 showcases a subset of these results, featuring a benchmark linear regression model alongside various ML models from Scenario 1, which utilize a combination of publicly accessible information and VLOG data.

The benchmark LR model performed significantly worse than the ML models, likely due to its limited capacity to capture non-linear relationships and complex interactions present in the data, as reflected by its negative testing R^2. Interestingly, we observe a case of overfitting for the training set using the kNN model, which suggests this model is not a favorite application. This is likely due to the model's sensitivity to sparse and noisy GPS-derived features and its severe reliance on local neighborhoods, which may be misleading in high-dimensional, sparse and unevenly distributed data. These limitations highlight the advantages of ensemble methods like Random Forest, which demonstrated more robust generalization under these conditions. Based on these performance metrics, we have chosen the RF model as the best model for

Table 5
Training performances of estimation models: Scenario 1 - with VLOG data.

	Training (266 samples)		Testing (66 samples)	
Estimation models	R^2	RMSE (log)	R^2	RMSE (log)
Linear regression (LR)	0.045	1.141	−0.037	1.775
Random forest (RF)	0.777	0.899	0.159	1.599
Gradient boosting trees (XGBoost)	0.428	2.073	0.098	2.742
Support vector regression (SVR)	0.370	2.285	0.020	2.978
K-nearest neighbors (kNN)	0.994	0.019	0.082	2.791
Neural networks (NN)	0.369	2.287	0.017	2.989

Table 6
Random Forest model training and testing performances of two scenarios.

	Training		Testing	
Scenario	R^2	RMSE (log)	R^2	RMSE (log)
Scenario 1 No VLOG	0.730	0.989	0.131	1.625
Scenario 1 VLOG data	0.777	0.899	0.159	1.599
Scenario 2 No VLOG	0.746	0.940	0.239	1.737
Scenario 2 VLOG data	0.741	0.949	0.242	1.734

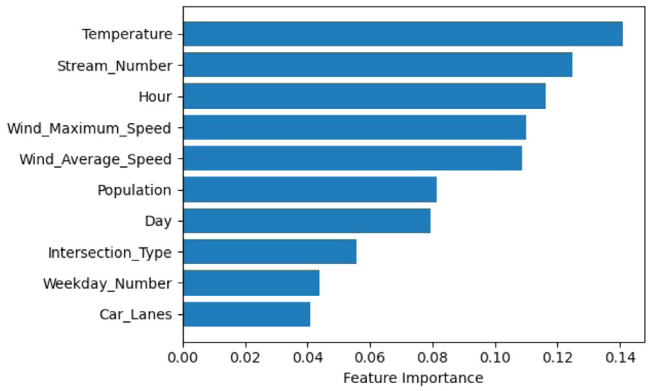

Fig. 5. Feature importance (Random Forest algorithm) from the previous work (Yuan et al., 2023).

further analysis. RF is typically resilient to outliers and can process them effectively without requiring explicit detection and treatment. Given the presence of extreme delay values in this dataset, it is plausible that RF outperforms other models in handling such anomalies. The current result demonstrates that by incorporating additional intersection controller and detection information, the model performance has increased, namely the R^2 value of the RF model can be elevated obviously (compared with a R^2 value of the RF model of 10 %), even when utilizing data from just 1 or 2 intersections (compared with the previous case of 18 intersections).

To provide specific scenarios, when using data from a single intersection (the 4-armed intersection in Delft), which had relatively limited total data samples but more comprehensive signal control and demand detection information for cars, bikes, pedestrians, buses, and trams, the model's performance improved regarding model fit and estimation accuracy of bike delay medians (as seen in Table 6).

Similarly, when using data from the two concerned intersections (in Scenario 2), certain data features in intersection ID 1, such as bus/tram signals and pedestrian detection information, had to be sacrificed to maintain data consistency. That means not all the influential features can be included in the estimation models. However, the interpretability of the machine learning model and the accuracy of delay estimation remained consistent in both scenarios. Under realistic data constraints (limited sample sizes and inherent noise in the raw data), this performance provides meaningful approximations of typical delay magnitudes. Although the numerical improvements in RMSE and R^2 appear modest in absolute terms, these changes are consistent with typical effect sizes in travel behavioral modeling where behavioral variance is high. These findings suggest that applying this machine learning model to a broader range of intersection data (with more samples and varying conditions) can enhance model accuracy and broaden its applicability.

In the comparative analysis of RF model performances across different datasets, the study presents an intriguing evaluation of the model's ability to predict outcomes when trained with the original data variables as used in Yuan et al. (2023) versus the case when supplemented with the VLOG data (see Table 6). The best model results are observed in Scenario 2 with the VLOG data, where it achieves the highest R^2 (elevated to 24.2 %) value compared to the other scenarios.

In this study, we explored the efficacy of incorporating additional VLOG data alongside traditional weather and temporal parameters in enhancing the predictive capabilities of the RF model. The results, while nuanced, offer valuable insights into model performance dynamics. Scenario 2's model, trained with the original data, demonstrated an exemplary fit to the training data, achieving an R^2 of 0.746, signifying a robust predictive alignment. When extended to the testing phase, although the R^2 showed a decrease, the model still maintained a respectable level of predictive accuracy. Furthermore, including the VLOG data presents a promising trend of improved (lower) RMSE values, albeit with slight variations. For instance, the RMSE (log) in Scenario 1 improved from 1.625 to 1.599 with the addition of VLOG data, a statistically significant improvement. The disparity between predicted and observed delay values across the two scenarios was found to be significantly different based on a paired *t*-test ($p = 0.0021$). This enhancement, albeit modest, underscores the potential of the VLOG data to contribute to the refinement and sophistication of predictive models, highlighting the value of integrating diverse data streams to capture a more holistic picture of the variables in the real world and thus to enhance both explanatory power and interpretability across scenarios. In the following sections, we will further explore the performance of each scenario.

5.2. Individual performance of delay distribution

To further study the differences in model fit between the two scenarios, we dive deeper into the model specification of the best-fitting models for Scenarios 1 and 2. In Section 5.2, delay distribution of Scenario 1 of one 4-armed intersection and Scenario 2 of combined two intersections are discussed in more depth.

5.2.1. Delay distribution of Scenario 1

Fig. 6 presents the delay distribution graphs for scenario 1. This figure illustrates a promising alignment between the predicted and actual bicycle delay times in Scenario 1. While the model demonstrates

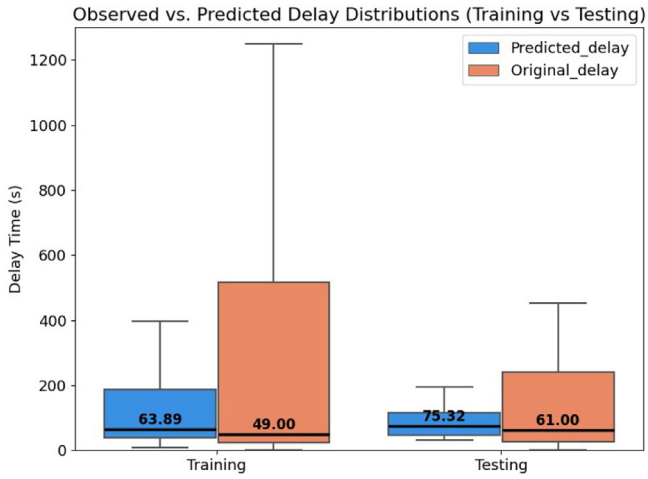

Fig. 6. Distribution of the predicted (in blue) and original (in red) delay time, Scenario 1.

a relatively good central tendency in predicting bicycle delay times, with training and test set median predictions at 63.89 and 75.32 s, respectively, we must admit that it notably overestimates shorter delays. This overestimation suggests a divergence from the actual median delay times of 49.00 and 61.00 s, indicating a potential underestimation of longer delay samples.

A more balanced prediction across the entire range of delay times is required to make the model applicable. To enhance its applicability, we are considering multiple avenues: expanding the dataset to include more diverse intersection types, refining our delay calculation algorithms, incorporating a more comprehensive range of variables, exploring advanced modeling techniques, and conducting a temporal and error analysis. These steps aim to develop a more nuanced understanding of delay distributions and improve the accuracy of our predictions across the entire spectrum of delay durations.

Fig. 7 further illustrates the performance of a predictive model in estimating delay times for bicycles, broken down by movement direction: right turn (R), straight through (T), and left turn (L). However, a loss of variance exists, suggesting that our model may not capture the full range of delay times as disparity exists (to a certain extent) between the individual predicted and original delays per direction. The comparison between the predicted and actual median delay times suggests that the model can generally reflect the delay ranges, with predictions closely matching the actual medians across all movement directions. For right turns, the model slightly overestimates the delay, with a predicted median of 61.82 s compared to an actual median of 45.00 s.

When going straight through, the model's overestimation is also observed, with predicted and actual medians at 54.51 and 41.00 s, respectively. For left turns, the predicted median is 118.55 s, moderately deviating from the actual median of 155.00 s. The test set results largely mirror the training set's results, indicating the model's consistency. The clustering of predicted values around the medians confirms the model's capacity to capture the central tendency of delay times for different traffic movements.

However, it becomes evident that the model underestimates the delays for left-turn movements, which implies that the model is particularly conservative when estimating delays for this movement. Specifically, the model prediction of 119.94 s is substantially lower than the observed delay of 244.00 s. This underestimation suggests that the model may not fully capture the efficiency with which cyclists are completing left turns, perhaps due to more favorable traffic conditions or quicker identification of safe gaps in traffic than the model anticipates. Adjustments to the model's assumptions about traffic interactions and cyclist behavior during left turns may be required to improve its predictive accuracy. Besides, this can also be attributed to the small sample population for this specific movement direction in the testing dataset (about 20 trip records for this 4-arm crossing), leading to this specific chance finding in statistics. It should also be noted that left-turning cyclists typically face more conflicts with motorized traffic and need to wait for larger or multiple safe gaps compared with through or right-turning movements, which inherently contributes to higher delays. This behavioral and infrastructural characteristic, combined with the small sample size, helps explain the observed underestimation. Further investigation into the data and refinement of the model's parameters could provide a more precise representation of the delays experienced by cyclists, particularly in the complex and variable scenarios that left turns often present.

5.2.2. Delay distribution of Scenario 2

Fig. 8 presents the predicted and actual bicycle delay times distribution for Scenario 2, considering a combined dataset from intersections ID 1 and 2. The graph reveals that the model maintains a commendable prediction accuracy despite omitting certain variables like bus/tram signal and bus/pedestrian detection due to the combination of intersections. While moderately overestimated, the predicted median delay times are relatively close to the actual medians across both intersections. For instance, the training set for intersection ID 1 shows a predicted median delay time of 59.90 s against an actual median of 53.00 s (13.02 %), and the test results indicate a predicted median of 78.55 s versus an actual median of 69.00 s (13.84 %). Intersection ID 2's training results have a predicted median of 28.86 s, which is a notable overestimation compared to the actual median of 22.50 s (28.27 % - note, a relatively large percentage might owe to a relatively small actual delay median). The test results show a predicted median of 37.64 s against an actual median of 17.50 s.

The findings indicate that the model captures the central trend of delay times with a consistent pattern across various scenarios and intersection conditions. While conservative, the model's current estimations provide a robust framework for estimating delays, ensuring that traffic systems can accommodate fluctuations beyond average conditions. However, it's acknowledged that the current level of overestimation may not be ideal for individual delay predictions. Improvements to the model could involve recalibrating the estimation process to align more closely with observed data, potentially integrating real-time traffic updates and cyclist feedback to refine predictions, particularly to capture the variance of delay distributions.

To enhance the practical application, we propose a two-fold approach: short-term application in traffic management as a provisional tool for planning, with a long-term strategy focusing on iterative model refinement. The immediate use would be in a strategic capacity, guiding the development of infrastructure and traffic signal adjustments, where conservative delay estimates would assist in designing resilient systems. Concurrently, we recommend an ongoing model improvement process, incorporating additional data sources (e.g., data from other intersections and other cities) and applying machine learning techniques to reduce prediction errors. This would improve individual delay estimations and enable the model to adapt to evolving urban landscapes and traffic patterns.

5.2.3. Delay medians considering all movement directions in Scenario 2

For intersection ID 1 using the testing set, the model estimation performance across all directions is marginally inferior compared to that in the training set, with the most notable deviation occurring for left turns where the predicted median (101.96 s) is significantly lower than the actual median (324.00 s) as shown in Table 7. This suggests a particular challenge in accurately predicting delays for left-turn movements at this intersection. Similar to Scenario 1, this can be attributed to the small sample population for this specific movement, and inherent behavioral and infrastructural characteristics for left turners, leading to this specific chance finding.

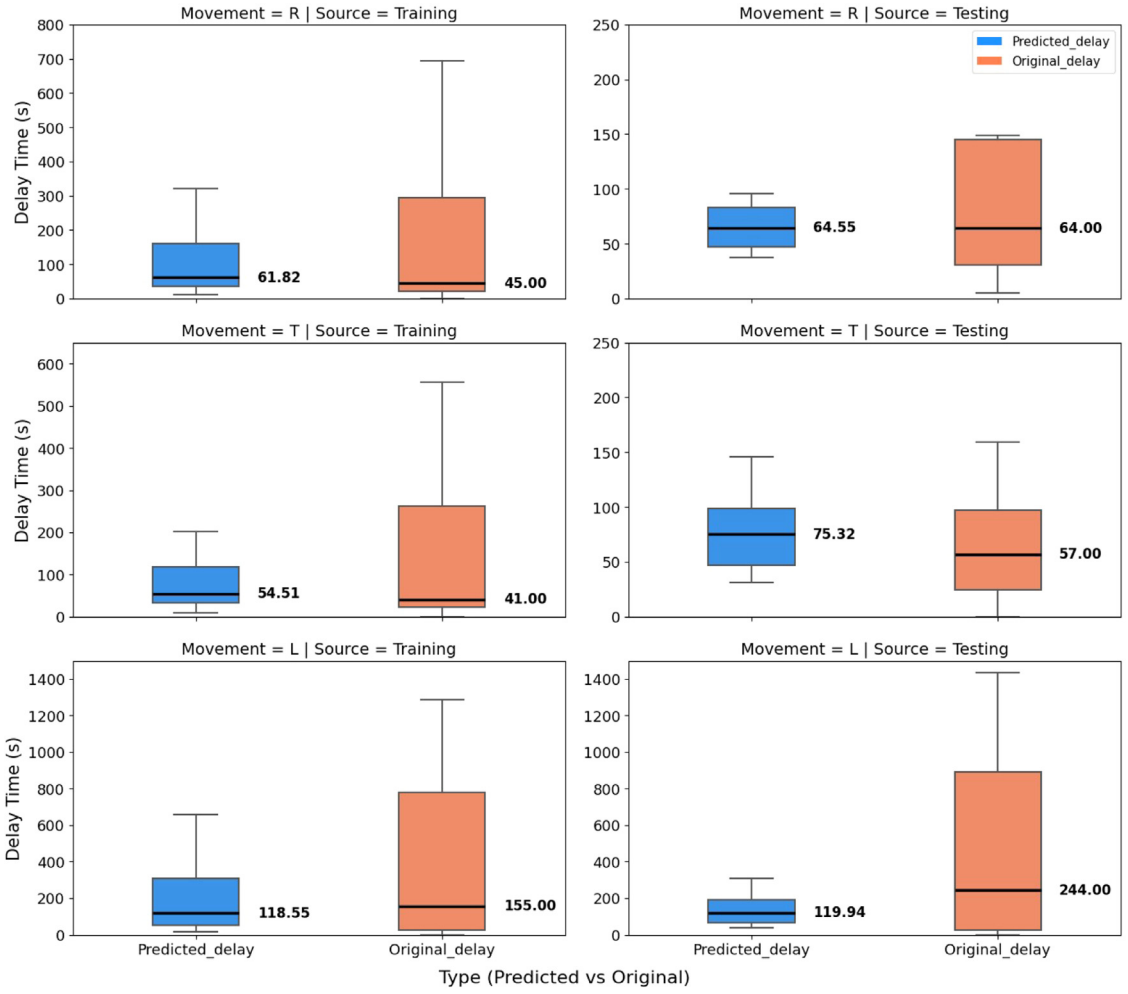

Fig. 7. Distribution of the predicted (in blue) and original (in red) delay time, Scenario 1 by different moving directions (R: right turn (Training: 65 trips; Testing: 16 trips), T: through going (Training: 110 trips; Testing: 28 trips), L: left turn (Training: 90 trips; Testing: 23 trips)).

Table 7
Delay medians for all movement directions of intersections 1&2 in Scenario 2.

		Right turn (R)			Through going (T)			Left turn (L)		
	median (s)	Predicted	Original	Sample	Predicted	Original	Sample	Predicted	Original	Sample
ID1	Training	55.95	50.00	65	48.64	43.00	110	157.94	161.00	90
	Testing	72.38	45.00	16	60.54	30.00	28	**101.96**	**324.00**	23
ID2	Training	21.28	17.00	38	**54.11**	**84.00**	37	28.08	22.00	62
	Testing	36.02	15.00	10	65.40	48.00	10	35.12	18.00	15

In contrast, for intersection ID 2 (T-junction) using the testing set, the predicted medians are much closer to the actual values for the three movement directions compared to the results for intersection ID 1 (4-armed intersection). Note that we observe a higher delay in through-going traffic (around 60 s) than the right-/left-turners (around 30 s). This is because traffic signals are primarily regulated through traffic (i.e., tidal commuting cycling flow between the university campus and the station). The training set for intersection ID 2 shows a better performance for the three movements with estimation errors of 25.18 %, 35.58 %, and 27.64 %.

5.3. Interpretation of feature importance

In Section 5.3, the interpretation of the features (independent variables) for both scenarios (including a SHAP analysis for Scenario 2) are discussed in more depth.

5.3.1. Feature importance of Scenario 1

In line with prior studies, our investigation assesses the impact of various factors on cycling delays (Fig. 9(a)). The temperature variable emerges as the foremost significant predictor within the RF model, corroborating earlier findings (Yuan et al., 2023). The average green light duration for cars within five-minute intervals ('Car_signal_AVG') ranks as the second most pivotal factor influencing cycling delays. The green light times for trams, buses, bicycles, and bike detection (request-green button and loop) over the same interval significantly contribute to these delays. This observation substantiates a close correlation between the control signal and various delay components, notably stop and control delays. It is a clear indicator that control signals play a pivotal role in influencing and reflecting the primary causes of delays at intersections.

Additionally, features such as intersection turning typology ('Stream_Number') and temporal elements like 'Weekday_number' and 'Hour' are also recognized among the top ten influential factors, consis-

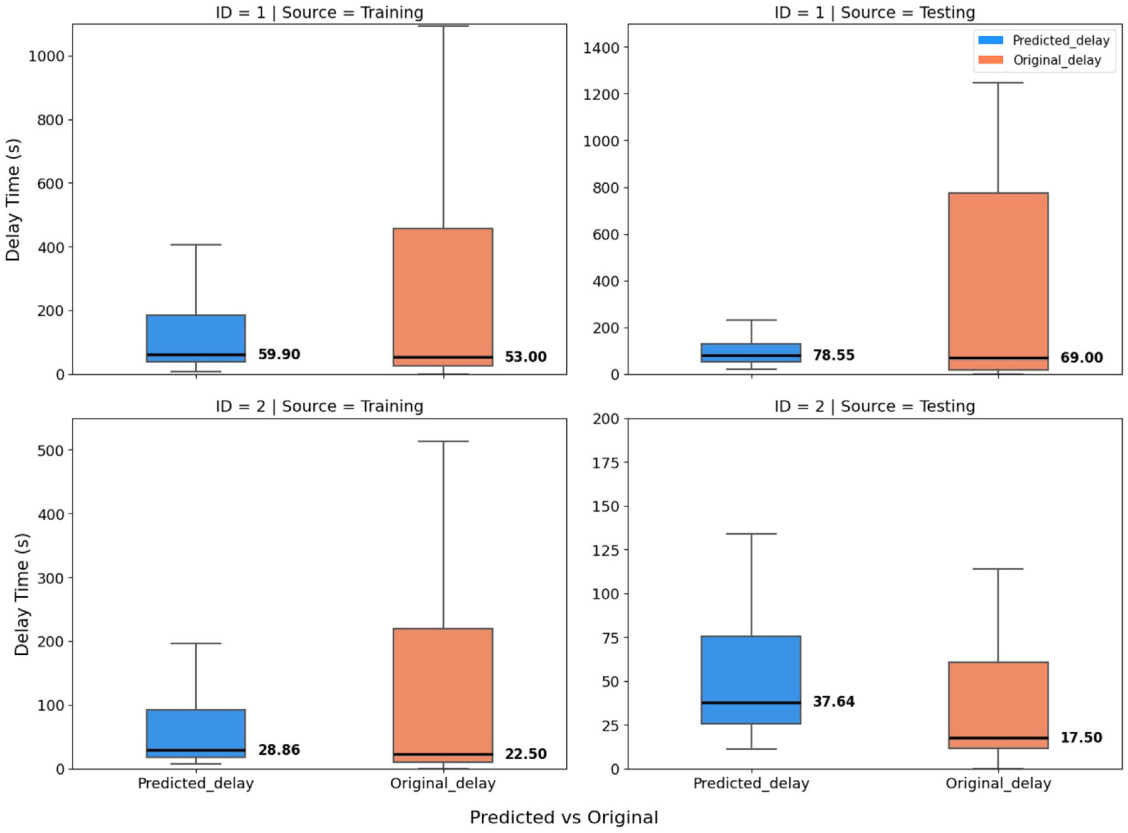

Fig. 8. Distribution of the predicted (in blue) and original (in red) delay time, Scenario 2 by intersection ID.

tent with previous research outcomes. Car appearance detected at the intersection during the 5-minute interval ('Car_det') is also found to be related to the travel delay. Overall, the current study highlights the impact of traffic signals and detection information on bicycle travel delays. Note that the detailed interpretation of various features will be discussed for scenario 2 due to its enhanced representativeness.

5.3.2. Feature importance of Scenario 2

In Scenario 2, the RF model's feature importance graph (Fig. 9(b)) highlights temperature as the most significant predictor in bicycle delay times, reinforcing previous findings from Scenario 1 and emphasizing the critical impact of weather factors on cycling conditions. Detection indicators for bicycles ('Bike_det_loops') and cars ('Car_det') rank as crucial variables, underscoring the importance of intersection dynamics on delay times. This diverges slightly from Scenario 1, where 'Car_signal_AVG' – the average green time for cars – was more prominent. Temporal features, such as the time of day ('Hour') and day of the week ('Weekday_Number'), remain consistently important across both scenarios, reflecting the influence of traffic patterns on delays. Compared with scenario 1, the bus signal feature is absent due to data sacrifice. Wind speed variables (mean and maximum speeds) fall in significance, suggesting that while they affect cycling conditions, their impact is secondary to temperature and intersection-related factors. The consistent prominence of 'Stream_Number' across both scenarios indicates the persistent effect of intersection-turning typology on delays. Overall, this model illustrates the interplay between weather conditions, traffic detection, and temporal factors in predicting bicycle delays at urban intersections.

5.3.3. Feature influence based on SHAP analysis

To gain insights into how different factors affect bicycle delays, we applied the SHAP (SHapley Additive exPlanations) package. This tool ranks the importance of each factor and shows how much each one contributes to the model's predictions individually. The influence of each factor is displayed in Fig. 10. The horizontal axis measures the strength of the impact, and the color signifies the value of the factor. The factors are listed from the most to the least important, and the dots' position to the left or right of the center line indicates whether a factor tends to increase or decrease the predicted bicycle delays.

5.3.4. Features with significant impact on delay estimation model

• Temperature

The SHAP analysis corroborates prior findings, highlighting temperature as a significant factor influencing cycling delays. Temperature may serve as a proxy for broader contextual conditions (e.g., weather-related impacts on riding conditions and cyclist behavior), which collectively influence delay outcomes. Warmer conditions tend to decrease delays, whereas colder temperatures, especially those falling below the annual Dutch average of 11 °C, have been observed to increase this quantity. This relationship is attributed to the adverse effects of cold weather on riding conditions and the consequent necessity for cyclists to proceed with increased caution. The consistency of these findings across studies emphasizes the critical role of temperature considerations in designing and managing cycling infrastructure.

• Bicycle request-green button (Bike_det_push)

The plot indicates that cyclists pressing the button to request a green signal usually experience a reduction in travel delay, as evidenced by a cluster of mixed-color dots on the left side showing negative SHAP values. This suggests an adequate response from the traffic signal system to the manual request, leading to shorter waiting times and, thus, delays. Conversely, isolated blue dots on the right with positive SHAP values suggest increased delays when the button is less frequently pressed, possibly due to non-optimized default signal timings. In other words, if the

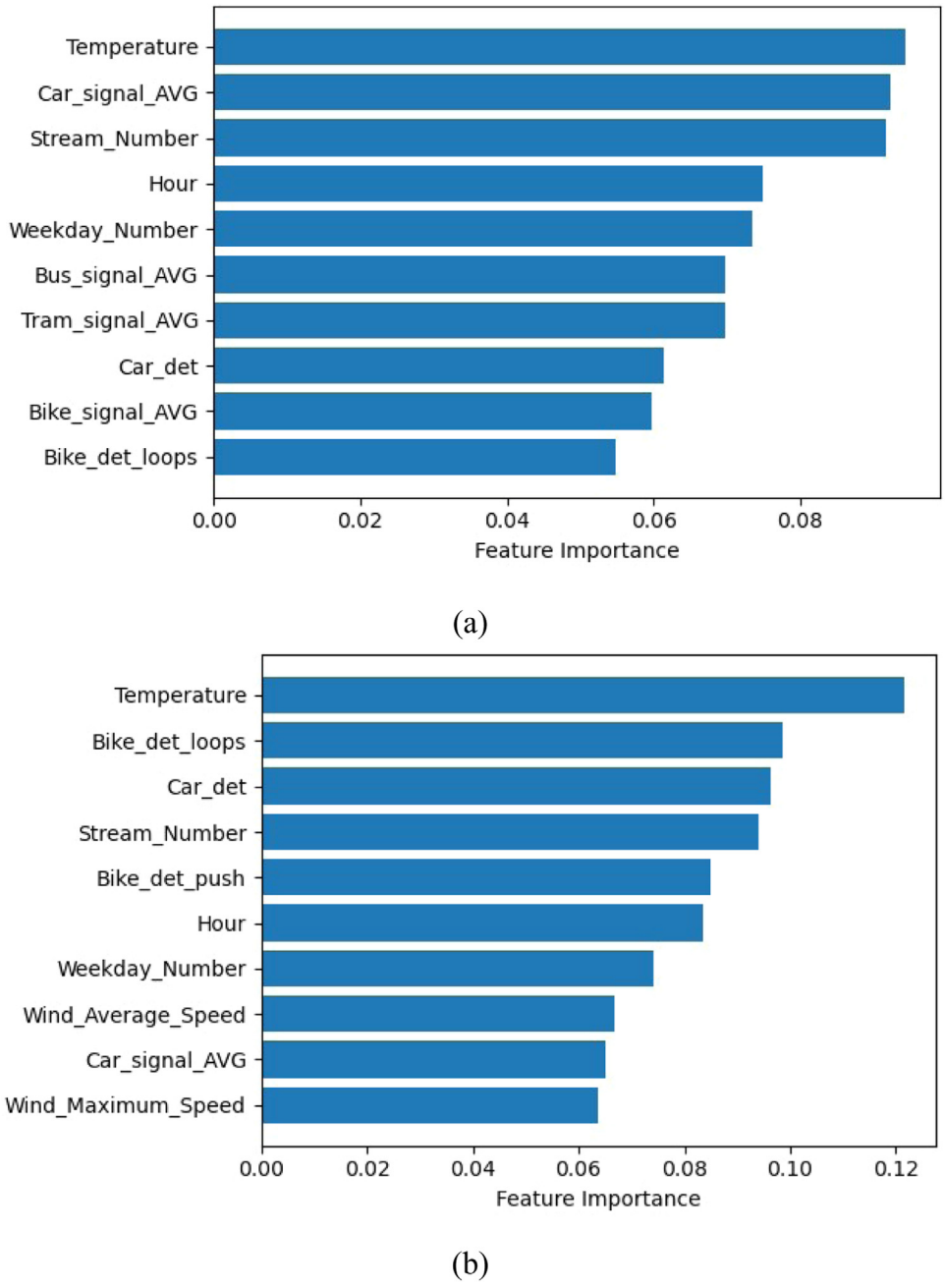

Fig. 9. Feature importance of the Random Forest algorithm for Scenario 1 (a), and Scenario 2 (b).

default timing of the traffic lights does not adequately account for the presence of bicycles, because it is primarily set up to manage vehicular flow, then cyclists may face longer delays unless they actively use the button to request a change in the signal. This highlights the importance of having a traffic signal system that is responsive to the needs of cyclists, both through manual input (the request-green button) and through automatic detection and signal adjustment.

• Bicycle loop detection (Bike_det_loops)

The predominance of blue and red dots on the right side with positive SHAP values reveals that detecting many bicycles often correlates with increased travel delays. This implies that detecting high bicycle traffic volumes is often associated with increased delays. Sparse blue dots on the left with negative SHAP values point to cases where detection with lighter traffic conditions is related to decreased delays.

• Car detection (Car_det)

A majority of data points with positive SHAP values indicate that higher frequencies of car detection are associated with increased bicycle delays, highlighting a potential congestion issue. The clustering of these values, especially the red/pink dots, suggests a significant impact of vehicular traffic on cycling delays at intersections. A minority of points with negative SHAP values suggests that lower volumes of vehicular traffic can decrease bicycle delays, emphasizing the need for adaptive signal systems that consider the flow of all commuters (e.g., car and bike travelers, as revealed by the model).

5.3.5. *Features with mild impact on delay estimation model*

• Wind speed (Wind_Average_Speed and Wind_Maximum_Speed)

The SHAP analysis from this study, with a smaller sample size, suggests only a slight influence of wind speed on cycling delays, a contrast to previous research with larger datasets (18 intersections –

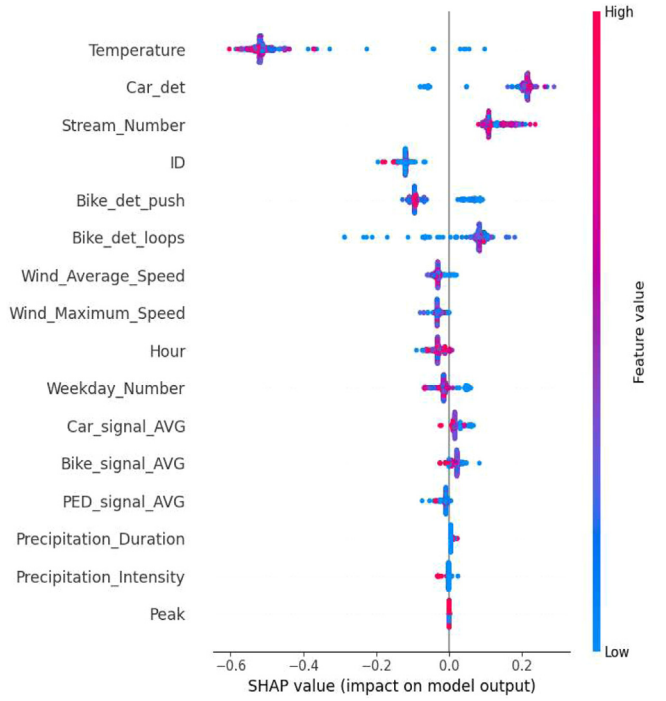

Fig. 10. SHAP summary plot of feature impact.

Yuan et al. 2023) that identified wind as a significant factor in increasing delays. This difference could be attributed to the reduced statistical power and variability inherent in a smaller dataset (as the two concerned intersections are located in the same city, and thus, the data is from the same weather station). Although our findings indicate a lesser impact, they do not negate the potential effects of wind conditions observed in larger-scale studies. Therefore, while wind speed's contribution to delay times may appear modest in the current context, it is still an important consideration in developing and managing cycling infrastructure, particularly in more comprehensive studies with larger datasets. Moreover, as we observed a high correlation between the average and maximum wind speed, the results are interpreted as reflecting the overall influence of wind conditions rather than emphasizing one specific variable.

- Average signal duration (Car_signal_AVG, Bike_signal_AVG, PED_signal_AVG):

The SHAP summary plot reveals that the average green-time durations for cars, bikes, and pedestrians have a more centralized cluster of SHAP values around the midpoint. This suggests a milder influence of control signals on bicycle delays than variables like car detection, manual bicycle green request, and bicycle loop detection, which exhibit more pronounced clusters away from the center. Hence, while signal timing affects delay, its impact appears less substantial than the presence of traffic demand and direct bicycle signal requests. Longer average green signal times for cars are generally linked to increased bicycle delays, pointing to a vehicle-centric traffic signal approach. Increasing bicycle signal durations do not consistently show a decrease in delays, which could indicate complex dynamics at intersections affecting cyclists. The pedestrian signal averages display a mixed relationship with bicycle delays, suggesting a variable impact that could depend on the particularities of each intersection's design and signal timing coordination.

This information holds value for cyclists, traffic planners, and policymakers alike. For instance, knowing that travel times are associated with increased delays under certain weather conditions can inform decisions about infrastructure improvements or traffic management strategies. Understanding the role of traffic demand detection (e.g., car and bicycle flows) and deploying control facilities smartly (e.g., the request-green buttons) can help in anticipating on-the-spot delays and formulate strategies to manage and reduce such delays.

5.4. Discussion of the results

In the complex landscape of intersection dynamics, a profound understanding of bicycle delays emerges as a key focal point. As bicycles increasingly become a popular mode of transportation, especially in urban areas, intersections serve as critical junctures where various modes intersect, necessitating a thorough comprehension of how bicycle delays impact overall traffic flow and efficiency. While we do not aim to develop the best accurate estimation model for monitoring individual bicycle delays at signalized intersections (e.g., minimizing prediction errors for individual delay samples) due to data scarcity and quality, instead, with the purpose of optimal utilization of the existing data sources, we show that one of the ML models, the RF model, can estimate and predict the average magnitude (regarding the central tendency, median and its distribution) of this crucial variable to an adequate level. Insights into various influential factors (reflecting weather, temporal information, topology, and traffic conditions) on bicycle delays from the estimation model pose great value to cyclists, urban planners, and policymakers. By closely examining turning maneuvers within intersections, we gain nuanced insights into the interplay of various traffic flows, which is especially crucial in a context where bicycle demand at intersections is notably high. This detailed examination allows us to discern the intricacies of each movement direction, understanding how different turns contribute to the overall traffic dynamics and how experiencing delays varies per movement direction. With this knowledge, prioritizing bicycle traffic becomes a possibility through strategies like introducing an on-site traffic warning system (via variable message signages), allocating more green time (via intersection controllers), or implementing dedicated cycle paths (via infrastructure design). However, such adaptations may impact other road users, potentially causing delays for cars, buses, or trams. Policymakers must weigh these considerations against equity concerns for all road users and align decisions with specific policy objectives and desired service quality. Our contribution to this decision-making process lies in unraveling information and key factors on bicycle delays. In addition, the model's insights can inform the development of dynamic route guidance tools that provide real-time information to cyclists based on historical analysis. For example, mobile applications could be developed to inform cyclists of expected delay times at intersections, allowing them to choose routes that minimize delays and improve their commuting experience.

Notably, we admit that there exists observed bias (overestimating short delays and underestimating longer ones, particularly for left-turning movements) in the estimation. This reflects a common trade-off in regression models trained on imbalanced data distributions. In our case, this is largely due to the under-representation of extreme delay cases in the dataset given data sparsity, and the behavioral complexity of left turns, which involve more conflict points and dynamic gap-acceptance behaviors than through or right-turn movement. From a strategic planning perspective, the model provides a reasonable approximation of average system performance and can identify relative differences across intersections or time periods. This supports decisions such as prioritizing infrastructure upgrades or adjusting signal control strategies at a network level. However, the same bias would be less appropriate for individual-level predictions, where accurate estimation of extreme values (e.g., very long delays) is critical. In such contexts, underestimating high-delay conditions could lead to under-investment in locations with more severe issues, whereas overestimating minor delays may cause overallocation of resources to less critical points. Recognizing this limitation, we suggest that future work incorporate more balanced or targeted data collection to better capture the tails of the delay distribution.

To mitigate and quantify these limitations, several methodological extensions can be considered. First, rebalancing techniques such as stratified sampling or weighted training could help address data imbalance across movement types. Second, expanding the dataset to cover more intersections and longer observation periods would improve representation of rare, high-delay cases. Third, incorporating additional explanatory variables related to intersection geometry, signal phasing, real-time traffic interactions, or conflicting vehicle flows may improve model sensitivity to left-turn-specific factors. Finally, diagnostic analyses such as residual error profiling and quantile-based error decomposition could be applied to explicitly assess and visualize model bias across different delay ranges and turning typologies. These analyses would allow for a clearer identification of systematic under- or overestimation patterns (e.g., for extreme or movement-specific delays) and help guide targeted model refinement. Together, these efforts would not only strengthen the credibility of movement-specific findings but also enhance the model's applicability in understanding the diversity of cycling delays under real-world conditions.

Expanding our analytical scope, the integration of the VLOG data marks a notable advancement compared with our previous work (Yuan et al., 2023). This additional dataset enriches our understanding and contributes to the refinement of the ML estimation models. The synergy between the VLOG data (control signals and flow detection) and the existing information (weather, temporal, and topology data) facilitates a more comprehensive assessment of intersection (in)efficiency. This holistic approach allows us to move beyond a generic analysis, considering specific movements and their impacts on the overall intersection performance.

One notable outcome of this enriched dataset is improving ML model fit. The details provided by VLOG data contribute to a more accurate representation of the complex dynamics (the model fit has doubled in Scenario 2 (testing case, using two intersections) compared with the case (of 18 intersections) without harnessing traffic control and detection information, 24.2 % vs. 10 %). This refinement is particularly evident in the reduction of prediction errors, signifying a higher precision in estimating delay magnitudes at local intersections and with a potential expansion to multiple intersections at a national level. As we delve into the directional aspects of delays via turning typology, the data allows us to distinguish between different movement directions with a level of granularity that was previously challenging to achieve. This serves as additional images for decision-making. Note that the final model fit of 24.2 % indicates that a substantial portion of variance remains unexplained, such values are typical for urban mobility models using inherently noisy and heterogeneous data sources such as GPS traces and signal data. This limitation largely reflects unobserved behavioral and contextual factors, including complex traffic interactions, intersection-specific geometries, and individual cyclist behavior. Note that the model should be applied cautiously in studies requiring detailed individual-level behavioral inference. Nevertheless, the model remains suitable for network-level planning and performance evaluation since it captures systematic spatiotemporal patterns and relative differences in bicycle delays across intersections - insights that are highly relevant for network-level signal optimization, infrastructure prioritization, and policy formulation.

6. Conclusion

The article enhances the capabilities and generalizability of the bicycle delay estimation model by incorporating control signals and detection information from signalized intersections. The findings illustrate the viability of estimating bicycle delays by considering the interplay among weather conditions, temporal factors, junction topology, and local traffic conditions. In particular, we confirm the crucial significance of temporal and weather variables, as well as turning typology, in anticipating and predicting delays under specific temporal and weather conditions. Moreover, insights gained from the estimation model underscore the impact of factors such as the frequency of request-green button usage by cyclists, resulting in reduced bicycle delays. Conversely, the extended average green duration for various modes of transportation, along with heightened demand for both cars and bicycles, is associated with increased bicycle delays.

This estimation application and its result should provide sufficient images for policymakers and cooperating authorities on average bicycle delay at specific intersections, for instance, to determine priority and function maps for bicycle users (as well as for car users). With this knowledge, prioritizing bicycle traffic becomes feasible through strategies such as introducing on-site traffic warning systems, allocating additional green time, establishing dedicated cycle paths, or developing dynamic route guidance tools (e.g., mobile apps) for cyclists. However, it is also crucial for policymakers to consider the potential impact on other road users and balance these concerns with equity considerations and desired service quality objectives.

With the availability of additional local traffic controller information (more intersection types and thus more samples), expanding the current estimation model holds the potential to enhance coverage regarding intersection types and traffic conditions. This expansion can lead to improved generalizability and accuracy in application, allowing traffic management measures to be tailored to specific and generic intersections.

In addition, efforts are needed to achieve a more balanced prediction across the entire range of delay times to enhance the model's applicability. This involves refining delay calculation algorithms (e.g., by selecting appropriate free-flow speed references, by improving trip geolocation accuracy via map-matching), incorporating a more comprehensive range of variables, and exploring advanced AI modeling techniques. Particular attention should be given to addressing model bias in extreme and movement-specific cases, such as the underestimation of longer delays and left-turn movements, by introducing rebalancing strategies, expanding datasets, error diagnostic analyses, and incorporating additional explanatory factors reflecting intersection geometry and traffic interactions. Additionally, a two-fold approach is proposed: short-term application in traffic management for planning purposes and a sustained, long-term strategy focusing on iterative model refinement. This includes recalibrating the estimation process, integrating real-time traffic updates and cyclist feedback, and incorporating additional data sources and machine learning techniques to reduce prediction errors and adapt to evolving urban landscapes and traffic patterns.

This study's implications underscore the importance of adaptive traffic systems that account for varied transportation needs and conditions, ultimately facilitating more efficient urban mobility. Policymakers and traffic engineers are encouraged to leverage these insights to optimize traffic flow and enhance safety for all road users.

Funding

No funding is available to this research.

Availability of data and materials

The GPS data and VLOG data are not publicly available due to the data non-disclosure agreement with the data providers. The derived datasets including all dependent and independent variables and the related codes are made available via the Mendeley data repository: 10.17632/gf5ygjstvn.2.

Declaration of competing interest

The authors declare that they have no known competing financial interests or personal relationships that could have appeared to influence the work reported in this paper.

CRediT authorship contribution statement

Yufei Yuan: Writing – review & editing, Writing – original draft, Visualization, Validation, Methodology, Investigation, Data curation, Conceptualization. **Kaiyi Wang:** Writing – review & editing, Writing – original draft, Validation, Investigation, Conceptualization. **Dorine Duives:** Writing – review & editing, Conceptualization. **Winnie Daamen:** Writing – review & editing. **Serge P. Hoogendoorn:** Writing – review & editing, Writing – original draft, Validation, Investigation, Conceptualization.

Acknowledgements

The authors would like to express many thanks to Rijkswaterstaat (the Dutch Ministry of Transportation) for providing the GPS cycling data from the Talking Bikes program, to Joost de Kruijf and Sascha Hoogendoorn-Lanser for acquiring the project on exploring bicycle trip data, and to De Gemeente Delft (Delft municipality) for providing the VLOG data.

References

Aurélien, G. (2019). Hands-on machine learning with Scikit-Learn, Keras, and TensorFlow: Concepts, tools, and techniques to build intelligent systems. *O'Reilly Media*. https://books.google.com.au/books?id=OCS1twEACAAJ.

Bagdatli, M. E. C., & Dokuz, A. S. (2021). Vehicle delay estimation at signalized intersections using machine learning algorithms. *Transportation Research Record, 2675*(9), 110–126. 10.1177/03611981211036874.

Balevski, E. I., & Lyubenov, D. (2018). A study of bicycle travel speed. *Proceedings of University of Ruse, 57*, 154–158.

Biau, G., & Scornet, E. (2016). A random forest guided tour. *Test (Madrid, Spain), 25*(2), 197–227. 10.1007/s11749-016-0481-7.

Brownlee, J. (2020). How to configure k-fold cross-validation. Retrieved Februrary 2024 from https://machinelearningmastery.com/how-to-configure-k-fold-cross-validation/

Buehler, R., Teoman, D., & Shelton, B. (2021). Promoting bicycling in car-oriented cities: Lessons from Washington, DC and Frankfurt Am Main. *Germany. Urban Science, 5*(3), 58. https://www.mdpi.com/2413-8851/5/3/58.

Chen, T., & Carlos, G. (2016). *XGBoost: A Scalable Tree Boosting System Proceedings of the 22nd ACM SIGKDD International Conference on Knowledge Discovery and Data Mining* 13 August 2016. 10.1145/2939672.2939785.

Cheng, C., Du, Y., Sun, L., & Ji, Y. (2016). Review on theoretical delay estimation model for signalized intersections. *Transport Reviews, 36*(4), 479–499. 10.1080/01441647.2015.1091048.

Fraser, S. D. S., & Lock, K. (2010). Cycling for transport and public health: A systematic review of the effect of the environment on cycling. *European Journal of Public Health, 21*(6), 738–743. 10.1093/eurpub/ckq145.

Gao, T., Daamen, W., Krishnakumari, P., & Hoogendoorn, S. (2024). Map-matching for cycling travel data in urban area. *IET Intelligent Transport Systems, 18*(11), 2178–2203. 10.1049/itr2.12567.

Gillis, D., Gautama, S., Van Gheluwe, C., Semanjski, I., Lopez, A. J., & Lauwers, D. (2020). Measuring delays for bicycles at signalized intersections using smartphone GPS tracking data. *ISPRS International Journal of Geo-Information, 9*(3), 174. https://www.mdpi.com/2220-9964/9/3/174.

Goodfellow, I., Bengio, Y., & Courville, A. (2016). *Deep learning*. MIT Press https://books.google.com.au/books?id=Np9SDQAAQBAJ.

Guo, N., Jiang, R., Wong, S. C., Hao, Q.-Y., Xue, S.-Q., & Hu, M.-B. (2021). Bicycle flow dynamics on wide roads: Experiments and simulation. *Transportation Research Part C: Emerging Technologies,, 125*, Article 103012. 10.1016/j.trc.2021.103012.

Hoogendoorn, S. P. (2005). Unified approach to estimating free speed distributions. *Transportation Research Part B: Methodological, 39*(8), 709–727. 10.1016/j.trb.2004.09.001.

Interstyles. (2021). *CuteView*. Retrieved 29 April 2024 from http://interstyles.nl/cuteview/ .

Kircher, K., Ihlström, J., Nygårdhs, S., & Ahlstrom, C. (2018). Cyclist efficiency and its dependence on infrastructure and usual speed. *Transportation Research Part F: Traffic Psychology and Behaviour, 54*, 148–158. 10.1016/j.trf.2018.02.002.

Lancering Nationale FietsTelWeek 2015. (2015). Retrieved 15 July 2023 from https://www.fietsersbond.nl/nieuws/lancering-nationale-fietstelweek-2015/

Leif, P. (2009). K-nearest Neighbor. Retrieved 15 July 2023 from http://www.scholarpedia.org/article/K-nearest_neighbor

Mobiliteits-Platform. (2020). Siemens en RingRing Verzamelen Fietsdata voor talking bikes Retrieved 15 July 2023 from https://www.mobiliteitsplatform.nl/artikel/siemens-en-ringring-verzamelen-fietsdata-voor-talking-bikes

Poliziani, C., Rupi, F., Schweizer, J., Saracco, M., & Capuano, D. (2022). Cyclist's waiting time estimation at intersections, a case study with GPS traces from Bologna. *Transportation Research Procedia, 62*, 325–332. 10.1016/j.trpro.2022.02.041.

Reggiani, G., Dabiri, A., Daamen, W., & Hoogendoorn, S. P. (2020). *Exploring the Potential of Neural Networks for Bicycle Travel Time Estimation. 13th Conference on Traffic and Granular Flow* 2 July 2020.

Rupi, F., Poliziani, C., & Schweizer, J. (2020). Analysing the dynamic performances of a bicycle network with a temporal analysis of GPS traces. *Case Studies on Transport Policy, 8*(3), 770–777. 10.1016/j.cstp.2020.05.007.

Smola, A. J., & Schölkopf, B. (2004). A tutorial on support vector regression. *Statistics and Computing, 14*(3), 199–222. 10.1023/B:STCO.0000035301.49549.88.

Strauss, J., & Miranda-Moreno, L. F. (2017). Speed, travel time and delay for intersections and road segments in the Montreal network using cyclist smartphone GPS data. *Transportation Research Part D: Transport and Environment, 57*, 155–171. 10.1016/j.trd.2017.09.001.

Ton, D., Cats, O., Duives, D., & Hoogendoorn, S. (2017). How do people cycle in Amsterdam, Netherlands?: Estimating cyclists' Route choice determinants with GPS data from an urban area. *Transportation Research Record, 2662*(1), 75–82. 10.3141/2662-09.

Velthuijsen, T. (2020). *Calculating cycling delay at signalized intersections using smartphone data*. University of Twente].

Vialis. (2020). V-log protocol en definities CROW.

West, R. M. (2021). Best practice in statistics: The use of log transformation. *Annals of Clinical Biochemistry, 59*(3), 162–165. 10.1177/00045632211050531.

Yang, F., Yao, Z., Cheng, Y., Ran, B., & Yang, D. (2016). Multimode trip information detection using personal trajectory data. *Journal of Intelligent Transportation Systems, 20*(5), 449–460. 10.1080/15472450.2016.1151791.

Yang, X., Huan, M., Si, B., Gao, L., & Guo, H. (2012). Crossing at a red light: Behavior of cyclists at urban intersections. *Discrete Dynamics in Nature and Society, 2012*(1), Article 490810. 10.1155/2012/490810.

Younes, H., Noland, R. B., Von Hagen, L. A., & Sinclair, J. (2023). Cycling during and after COVID: Has there been a boom in activity? *Transportation Research Part F: Traffic Psychology and Behaviour, 99*, 71–82. 10.1016/j.trf.2023.09.017.

Yuan, Y., Daamen, W., Duives, D., & Hoogendoorn, S.P. (2016). Comparison of Three Algorithms for Real-Time Pedestrian State Estimation - Supporting a Monitoring Dashboard for Large-Scale Events. In Proceedings of 2016 IEEE 19th International Conference on Intelligent Transportation Systems (ITSC).See: https://ieeexplore.ieee.org/document/7795974

Yuan, Y., Goñi-Ros, B., Poppe, M., Daamen, W., & Hoogendoorn, S. P. (2019). Analysis of bicycle headway distribution, saturation flow and capacity at a signalized intersection using empirical trajectory data. *Transportation Research Record, 2673*(6), 10–21. 10.1177/0361198119839976.

Yuan, Y., Wang, K., Duives, D., Hoogendoorn, S., Hoogendoorn-Lanser, S., & Lindeman, R. (2023). Bicycle data-driven application framework: A Dutch case study on machine learning-based Bicycle delay estimation at signalized intersections using nationwide sparse GPS data. *Sensors, 23*(24), 9664. https://www.mdpi.com/1424-8220/23/24/9664.